

Chemisorption tobacco mosaic virus removal from aqueous solutions and study of virus interaction with active chemisorbent surface by infrared spectroscopy

Olga V. Arapova,^{*a} Galina N. Bondarenko,^a Olga V. Bukhtenko,^a Marina V. Arkhipenko,^b Mark V. Tsodikov^a and Alexander I. Netrusov^{a,b,c}

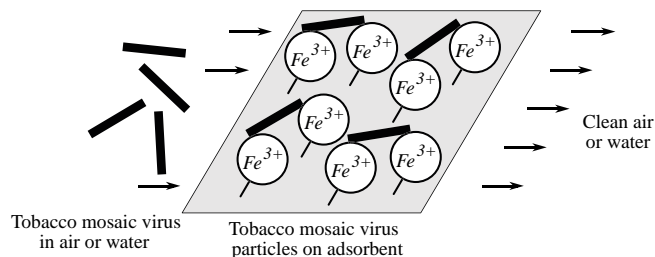
^a A. V. Topchiev Institute of Petrochemical Synthesis, Russian Academy of Sciences, 119991 Moscow, Russian Federation. E-mail: arapova@ips.ac.ru

^b Department of Biology, M. V. Lomonosov Moscow State University, 119991 Moscow, Russian Federation

^c Department of Biology and Biotechnology, National Research University Higher School of Economics (HSE University), 101000 Moscow, Russian Federation

DOI: 10.1016/j.mencom.2022.11.041

The interaction of the tobacco mosaic virus with the active surface of an iron-containing adsorbent obtained from lignin by the plasma-catalytic method was studied by IR spectroscopy. The results revealed decomposition of the virus into protein molecules and RNA reacting with the lignin surface *via* oxygen atoms during the binding of the virus to the sorbent surface. It was assumed that oxygen carboxylate groups interrelate with nanosized iron clusters incorporated into the adsorbent surface structure.



Keywords: lignin, adsorbent, tobacco mosaic virus, protein, IR spectroscopy.

One of the most important modern problems is the development of effective ways to remove viruses from their habitat. Viruses are non-cellular infectious agents that can reproduce only inside the cells of living organisms, from plants and animals to bacteria and archaea.^{1–4} It is the development of adsorbents possessing selectivity and efficiency in virus removal from its environment, which is one of the tasks in this field. One of the promising sources of the carbon adsorbents is lignin, its processing allows one to obtain hydrocarbon compounds and adsorbents.^{5–8} Previously, using lignin of wood origin we developed a carbon adsorbent with a monomodal porous structure ($d = 3.8$ nm) containing clusters of iron oxide (Fe^{3+}) 4–6 nm in size. High chemisorption activity of the sorbent with respect to oxygen-containing aromatic compounds was demonstrated by the example of cresol sorption.⁹ Here we report for the first time the results of tobacco mosaic virus (TMV) chemisorption using a dry or wet adsorbent produced from modified natural lignin by plasma-catalytic conversion as a model.

TMV particles were grown on tobacco plants by the standard technique;¹ samples with working concentration of $300 \mu\text{g ml}^{-1}$ in a 10 mM Tris–HCl buffer (pH 7.5) were prepared.¹⁰ Three different columns with the carrier, porous adsorbent obtained from wood lignin, were produced according to the method described earlier.¹ Virus particles were applied to pre-wetted (1) or dry (2 and 3) columns and column 3 was washed with sterile saline solution after the virus application. In total, 9 fractions were collected after TMV applications; the virus protein content in each sample was measured using the NanoDrop 2000 Spectrophotometer (Thermo Scientific, Germany) and gel electrophoresis. Table 1 shows the results of the determination of protein and virus in the fractions collected from columns 1–3. As can be seen from the Table 1,

TMV protein has not been detected in any of the collected fractions, this indicates that TMV particles have been completely sorbed on the surface of the chemisorbent.

To prove these results, the protein content in the collected fractions was analyzed by the protein electrophoresis, which also did not show any detectable protein concentrations in all the samples collected after the virus passed through the adsorbent (this data is not provided). The obtained results revealed the high selectivity of the tested adsorbent in relation to the virus sorption. The adsorbed viral preparation was not washed out of the adsorbent when the columns have been rinsed either with water (fractions C1–C3 and M1–M3) or with sterile saline (0.85% NaCl; fractions CC1–CC3). The virus absence in the samples, which passed through the column with an adsorbent pre-wetted by water, suggests that the TMV virus particles interact with the active centers of the adsorbent surface.

To verify the data obtained on the sorption and inactivation of TMV proteins on chemisorbent, IR spectra of the initial sorbent, the sorbent with the applied TMV and protein (bovine serum albumin, BSA) were measured in attenuated total reflectance (ATR) mode. IR spectra of a TMV aqueous solution and water were obtained in the ATR mode for samples in the form of

Table 1 Protein content ($\mu\text{g ml}^{-1}$) in the washing fractions after TMV sorption on columns with modified lignin.

Columns	1 (wet)	2 (dry)	3 (dry + NaCl)
Fractions	M1 \leq 0.1	C1 \leq 0.1	CC1 \leq 0.1
	M2 \leq 0.1	C2 \leq 0.1	CC2 \leq 0.1
	M3 \leq 0.1	C3 \leq 0.1	CC3 \leq 0.1
Source test TMV	300		

droplets. The IR spectra of the sorbent and the sorbent with adsorbates (virus and protein) were qualitatively similar. Therefore, differential spectra of adsorbates were gained, and then the spectra were reduced to the same baseline and to the same intensities of the normalization bands.

Figure 1 shows the differential TMV spectrum obtained by subtracting the water spectrum from the spectrum of aqueous virus suspension previously reduced to the same baseline and normalized to the 3345 cm^{-1} band. The second ATR spectrum was recorded for the BSA dry powder. The spectrum of the virus reflects the structure characteristic of RNA nitrogenous bases, apparently, cytosine and/or purine nucleotides, inasmuch as three bands at 3350 , 3250 and 3177 cm^{-1} correspond to the primary amino group inherent of these nucleotides. In addition, the other bands characteristic of nucleotides, appear in the spectrum of the virus: 3052 cm^{-1} ($\nu_{\text{H-C}}$), 1545 cm^{-1} ($\nu_{\text{C=C-O}}$), 1018 cm^{-1} ($\nu_{\text{N-C}}$), 875 and 787 cm^{-1} ($\delta_{\text{H-C}}$). The band at 1258 cm^{-1} matches good with the stretching bands from P=O bonds in the phosphate structure of RNA; several bands in the region of 1160 – 1090 cm^{-1} characterize C–O bonds in pentose residues. The protein shell, in which the virus should be located, is characterized by very weak split bands from the peptide bonds in the area of 1680 – 1500 cm^{-1} . However, sufficiently intense bands from amino groups (3400 – 3170 cm^{-1}), intense bands from saturated C–H bonds (2923 and 2856 cm^{-1}) and an intense band at 1745 cm^{-1} from stretching C=O bonds in the carboxyl group indicate that the low intensity of the bands from peptide groups is due to the very low molecular weight of the polypeptide; whereas intense bands from the acidic carboxyl group and amino group correspond to the terminal groups of the amino acid chain of the protein macromolecule. Intense bands from saturated C–H bonds can be attributed to such amino acids as valine, leucine, isoleucine and lysine. Finalising the description of the virus IR spectrum[†] we can conclude that all the spectral features of RNA and protein envelope are well manifested in the obtained IR spectrum of the TMV aqueous solution, though the protein in the virus has fairly short polypeptide chains with the large number of terminal groups of amino acids ($-\text{NH}_2$ and $-\text{COOH}$).

The second spectrum (see Figure 1) of the dry BSA protein represents a typical spectrum of protein molecules with well manifested bands from peptide bonds: 3292 cm^{-1} ($\nu_{\text{N-H}}$) and bands at 1646 , 1531 cm^{-1} and a weak broad band at 1233 cm^{-1} characterizing the secondary amide. The terminal protein amino

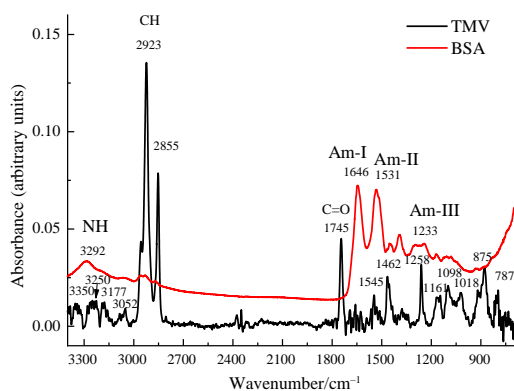


Figure 1 TMV – differential IR spectrum of the aqueous virus solution after subtracting the water spectrum; BSA – IR spectrum of the dry protein.

[†] IR spectra of the initial sorbent and the sorbent with the applied TMV were recorded in the attenuated total reflectance (ATR) mode (ZnSe crystal, 50 scans, resolution 2 cm^{-1} , range 600 – 4000 cm^{-1} , the IFS-66v Spectrometer, Bruker). IR spectra of TMV aqueous solution and water were measured in the ATR mode with identical registration parameters for samples in a droplet form.

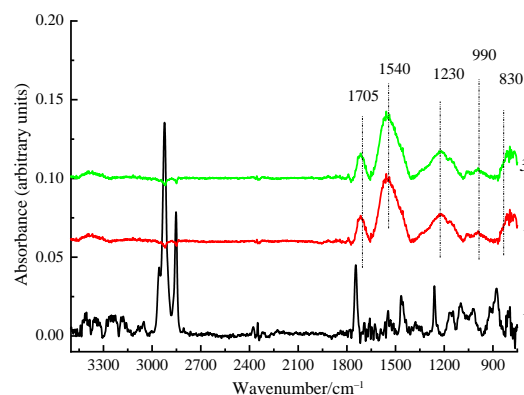


Figure 2 The differential IR spectra: 1 – TMV (the aqueous virus solution minus the water spectrum), 2 – sorbent with virus minus adsorbent spectrum and 3 – dry sorbent with virus minus sorbent spectrum.

acids groups are completely absent in this spectrum, *i.e.*, the polymer in question has a sufficiently high molecular weight.

Figure 2 shows the differential spectra of the virus on the carbon carrier surface in comparison with the spectrum of the virus described above. Differential spectra were obtained by subtracting the carrier spectrum from the corresponding carrier spectrum with sorbate, previously reduced to the same baselines and normalized to the 1054 cm^{-1} band of the adsorbent spectrum. The spectra 2 and 3 of the virus are very similar and exhibit all the characteristics of the spectrum 1 of the virus, but at the same time, the bands are much wider and shifted towards the long wavenumbers as a result of binding by noncovalent bonds to the sorbent surface. The band at 1745 cm^{-1} from the carboxylate group in spectrum 1 shifts to 1705 cm^{-1} in the spectra 2 and 3 of the adsorbed virus; the band at 1258 cm^{-1} from P=O expands and shifts to 1230 cm^{-1} . Particularly noteworthy is the sharp increase in the integral intensity of the 1540 cm^{-1} band in the spectrum of the virus adsorbed on the carbon carrier. This is due to the superposition of two types of the bands – from purine and pyrimidine nitrogenous bases in RNA (1545 cm^{-1}) and from the carboxylate ion $-\text{C}(\text{O})\text{O}^-$ (absorption region 1500 – 1600 cm^{-1}) – that resulted from the interaction between carboxyl group from a low molecular weight protein molecule of the virus envelope (band at 1745 cm^{-1}) and an oxidized form of iron in the adsorbent. It can be assumed that it is the ionic binding between the carboxyl group in the composition of the virus and the nanosized metal oxide in the adsorbent composition that ensures sufficient virus sorption on the carbon sorbent surface. The absence of the bands from CH bonds (2950 – 2840 cm^{-1}) in amino acids in the spectra 2 and 3 (see Figure 2) is due to two factors: the amphiphilicity of protein polymer molecules and the spectra registration conditions. Spectrum 1 was recorded from the surface of an aqueous solution droplet where hydrophobic (alkyl) groups are concentrated on the surface due to the amphiphilicity of protein molecules. Spectra 2 and 3 were recorded for the solid phase where the protein amphiphilic properties are not manifested.

Thus, the obtained results prove conclusively the active virus chemisorption on the adsorbent surface which inevitably results in the inactivation of the virus. Iron-containing particles immobilized on the initial lignin surface and present in the carbon residue can be used as active surface centers binding the surface proteins of viral particles.

Our further work will focus on determining the maximum concentrations of the adsorbent surface saturation with the virus and studying the structure of the adsorbed TMV particle in order to clarify the possible mechanism of the virus interaction with the active surface of the iron-containing adsorbent using electron microscopy and Mössbauer spectroscopy.

References

- 1 E. V. Koonin, T. G. Senkevich and V. V. Dolja, *Biol. Direct.*, 2006, **1**, 29.
- 2 J. S. Towner, M. L. Khristova, T. K. Sealy, M. J. Vincent, B. R. Erickson, D. E. Bawiec, A. L. Hartman, J. A. Corner, S. R. Zaki, U. Ströher, F. Gomes da Silva, F. del Castillo, P. E. Rollin, T. G. Ksiazek and S. T. Nichol, *J. Virol.*, 2006, **80**, 6497.
- 3 A. N. H. Creager and G. J. Morgan, *Isis*, 2008, **99**, 239.
- 4 E. C. Holmes, *PLoS Biol.*, 2007, **5**, 278.
- 5 O. V. Arapova, M. V. Tsodikov, A. V. Chistyakov and G. I. Konstantinov, *Chem. Eng. Trans.*, 2017, **57**, 223.
- 6 M. V. Tsodikov, S. A. Nikolaev, A. V. Chistyakov, O. V. Bukhtenko and A. A. Fomkin, *Microporous Mesoporous Mater.*, 2020, **298**, 110089.
- 7 L. M. Kustov, A. L. Tarasov and A. L. Kustov, *Mendeleev Commun.*, 2020, **30**, 76.
- 8 L. M. Kustov, A. L. Tarasov, V. D. Nissenbaum and A. L. Kustov, *Mendeleev Commun.*, 2021, **31**, 376.
- 9 G. N. Bondarenko, A. S. Kolbeshin, E. Yu. Liberman, A. V. Chistyakov, V. I. Pasevin and M. V. Tsodikov, *Pet. Chem.*, 2021, **61**, 81 (*Neftekhimiya*, 2021, **61**, 92).
- 10 E. A. Trifonova, N. A. Nikitin, M. P. Kirpichnikov, O. V. Karpova and J. G. Atabekov, *Moscow Univ. Biol. Sci. Bull.*, 2015, **70**, 194 (*Vestn. Mosk. Univ., Biol.*, 2015, no. 4, 46).

Received: 31st March 2022; Com. 22/6853